Cell Reports, Volume *22*

Supplemental Information

α Cell Function and Gene Expression Are Compromised in Type 1 Diabetes

Marcela Brissova, Rachana Haliyur, Diane Saunders, Shristi Shrestha, Chunhua Dai, David M. Blodgett, Rita Bottino, Martha Campbell-Thompson, Radhika Aramandla, Gregory Poffenberger, Jill Lindner, Fong Cheng Pan, Matthias G. von Herrath, Dale L. Greiner, Leonard D. Shultz, May Sanyoura, Louis H. Philipson, Mark Atkinson, David M. Harlan, Shawn E. Levy, Nripesh Prasad, Roland Stein, and Alvin C. Powers

SUPPLEMENTAL EXPERIMENTAL PROCEDURES

Contact for reagent and resource sharing

Further information and requests for resources and reagents should be directed to and will be fulfilled by the lead contact, Marcela Brissova (marcela.brissova@vanderbilt.edu) or Alvin Powers (al.powers@vanderbilt.edu).

DNA sequencing

DNA samples were sequenced using a custom designed next-generation sequencing (NGS) targeted panel that includes 148 genes implicated in monogenic forms of diabetes (neonatal diabetes and MODY), insulin resistance, lipodystrophy, obesity, rare syndromic forms of diabetes, and diabetes candidate genes (Alkorta-Aranburu et al., 2016). The targeted NGS approach was based on the SureSelect enrichment (Agilent Technologies) protocol followed by MiSeq Illumina NGS. Data quality was assessed using FastQC. Variants were called using The Genome Analysis Toolkit (GATK) HaploTypeCaller v3.3 and assigned to the transcripts of interest. Variants were then annotated in regards to their positions in transcripts of interest, position relative to the coding sequence, consequence for the protein or mRNA and a collection of direct and indirect evidentiary tools and databases including NCBI dbSNP, 1000 Genomes Project, Exome Sequencing Project (ESP), GERP, Conseq, PolyPhen-2, SIFT and the Human Gene Mutation Database (HGMD). All variants were interpreted according to the guidelines of the American College of Medical Genetics. All likely pathogenic variants identified by NGS were confirmed by Sanger sequencing.

Measurement of endocrine cell populations

Islet dissociation and intracellular antibody staining used a previously described protocol (Blodgett et al., 2015). Anti-insulin (Gallus Immunotech), anti-chicken allophycocyanin, (Jackson ImmunoResearch), anti-glucagon (Sigma-Aldrich) conjugated with Zenon Pacific Blue (Invitrogen), and anti-somatostatin (LSBio) conjugated with Zenon Alexa Fluor 488 (Invitrogen) were used to stain β, α, and δ cells, respectively (**Resources Table**). Dissociated islet cell preparations were analyzed using a BD Biosciences FACS Aria II Cell Sorter (University of Massachusetts Medical School Flow Core Laboratory). Cellular debris was eliminated from islet preparations using a forward scatter versus side scatter size gate.

Assessment of pancreatic islet function *in vitro*

Function of islets from T1D donors and normal controls (**Tables 1** and **S1**) was studied in a dynamic cell perifusion system at a perifusate flow rate of 1 mL/min (Kayton et al., 2015). The effluent was collected at 3-minute intervals using an automatic fraction collector. Insulin and glucagon concentrations in each perifusion fraction and islet extracts were measured by radioimmunoassay (Millipore).

qRT-PCR of isolated pancreatic islets

Quantitative reverse transcription polymerase chain reaction (qRT-PCR) was performed using the primer-probe approach from Applied Biosystems (Life Technologies) with *18S* and *ACTB* endogenous controls using Minimum Information for Publication of Quantitative Real-Time PCR Experiments (MIQE) guidelines as described (Brissova et al., 2014). All primers are listed in **Resources Table**. Gene expression in recent-onset T1D donors was compared to normal controls (**Tables 1** and **S1**). We were able to detect *INS* mRNA in T1D islets by RT-PCR and found that it was reduced to 19±7% compared to controls.

α cell sorting by flow cytometry for RNA-sequencing
Human islets were dispersed using a modified protocol as described previously (Aamodt et al., 2016). Briefly, 0.025% trypsin was used to disperse cells and reaction was quenched with modified RPMI medium (10% FBS, 1% Penn/Strep, 5 mM glucose). Cells were washed in the same medium and counted on a hemocytometer, then transferred to FACS buffer (2 mM EDTA, 2% FBS, 1X PBS). Indirect antibody labeling was completed via two sequential incubation periods at 4C, with one wash in FACS buffer following each incubation. Primary and secondary antibodies, listed in **Resources Table**, have been characterized previously and used to isolate high-quality RNA from α cells (Dorrell et al., 2016). Appropriate single color compensation controls were run alongside samples. Prior to sorting, propidium iodide (0.05 ug/100,000 cells; BD Biosciences, San Jose, CA) was added to samples for non-viable cell exclusion. Flow analysis was performed using an LSRFortessa cell analyzer (BD Biosciences), and a FACSAria III cell sorter (BD Biosciences) was used for FACS. Analysis of flow cytometry data was completed using FlowJo 10.1.5 (Tree Star).

Islet transplantation and assessment of grafts
T1D islets were transplanted into immunodeficient 10-12 week old NOD-*scid*-*IL2rγ*^{null} (NSG) male mice. Human islets from three normal donors with an average age of 37 years (range from 20 to 53 years) and average BMI of 25.1 (range from 21.7 to 28.2) were obtained through IIDP (**Table S1**). NSG mice were transplanted beneath the renal capsule with 500 – 600 normal or T1D islet equivalents (prepared as described above). Each set of islets was transplanted into 7-8 mice. Islets were allowed to engraft for 1 month and then mice were randomized for an additional 1-month treatment with either phosphate buffered saline (PBS) or exendin-4 (Ex), which were administered using an Alzet minipump (model 1004 with a pump volume of 100 μL, Durect Corporation). Ex-4 (California Peptide) was reconstituted in PBS without Ca^{2+} and Mg^{2+} and loaded into Alzet pump at concentration of 0.9 mg/mL. Ex-4 in plasma was measured by EIA (Phoenix Pharmaceuticals) and reached concentration of 4.4 ± 0.2 ng/mL (n=8 mice). Insulin secretion in transplanted human islets was assessed by intraperitoneal administration of glucose (2 g/kg of body weight) and arginine (2 g/kg of body weight) prior to and after Ex-4/PBS treatment. Human insulin in plasma was measured by species-specific radioimmunoassay (Millipore).

Immunohistochemical analysis
Immunohistochemical analysis of pancreas was performed on serial 5-μm cryosections from multiple blocks from head, body and tail regions as described (Brissova et al., 2014). Kidneys bearing islet transplants were collected and then 5-μm cryosections from 5-6 different depths of each graft were labeled for immunofluorescence as described (Brissova et al., 2014). Primary antibodies to all antigens and their working dilutions are listed in the **Resources Table**. The antigens were visualized using appropriate secondary antibodies listed in the **Resources Table**. Tyramide Signal Amplification (Perkin Elmer) was used to visualize ARX and NKX2.2 labeling. Digital images were acquired with a Zeiss LSM510 META laser scanning confocal microscope (Carl Zeiss).

RNA-sequencing
Sorted α cells (5,000-125,000) were added to 200 μL lysis/binding solution in the RNAqueous micro-scale phenol-free total RNA isolation kit (Ambion). Trace DNA was removed with TURBO DNA-free (Ambion), RNA integrity was evaluated (Agilent 2100 Bioanalyzer; control, 8.36±0.22 RIN, n=5 donors; T1D, 7.97±0.32 RIN, n=3 donors), and high-integrity total RNA was amplified (Ovation system; NuGen Technologies) per standard protocol as described previously (Brissova et al., 2014). Amplified cDNA was sheared to target 200bp fragment size and libraries were

prepared using NEBNext DNA Library Prep (New England BioLabs). 50bp Paired End (PE) sequencing was performed on an Illumina HiSeq 2500 using traditional Illumina methods (Malone and Oliver, 2011) to generate approximately 50 million reads per sample. Raw reads were mapped to the reference human genome hg19 using TopHat v2.1 (Trapnell et al., 2009). Aligned reads were then imported onto the Avadis NGS analysis platform (Strand life Sciences) and filtered based on read quality followed by read statistics to remove duplicates. Transcript abundance was quantified using the TMM (Trimmed Mean of M-values) algorithm (Dillies et al., 2012; Robinson and Oshlack, 2010) as the normalization method.

Quantification of cellular protein expression

Histopathology reviews were conducted on the whole slide digital images. Protein expression of nuclear factors in α and β cells was quantified using MetaMorph 7.1 imaging software (Molecular Devices) using manual cell counting (Brissova et al., 2014) where an average of 351±73 α cells and 861±141 β cells were counted per normal donor (n=7), and average of 718±50 α cells and 45±17 β cells were counted per T1D donor (n=4) for each transcription factor.

RNA-sequencing analysis

Genes with normalized expression values less than 25 were removed prior to differential expression analysis between control and T1D groups. Fold change (cutoff ≥ ±1.5) was calculated based on p-value estimated by z-score calculations (cutoff 0.05) as determined by Benjamini Hochberg false discovery rate (FDR) correction of 0.05 (Benjamini and Hochberg, 1995). Differentially expressed genes were further analyzed through Ingenuity Pathway Analysis (IPA, Qiagen) (**Figure S4C**, **Table S3**) and Gene Ontology (GO) analysis using DAVID v6.8 (Huang et al., 2009) (**Figures 4B** and **S4D**, **Table S4**).

RESOURCES TABLE

REAGENT or RESOURCE	SOURCE	IDENTIFIER
Antibodies		
Rabbit anti-ARX (1:1000)	Beta Cell Biology Consortium (BCBC)/Patrick Collombat	N/A
Rabbit anti-Glucagon (1:200)	Cell Signaling	Cat# 2760; RRID: AB_659831
Mouse anti-Glucagon (1:500)	Abcam	Cat# ab10988; RRID: AB_297642
Mouse anti-Glucagon- Pacific Blue (1:600; flow cytometry)	Sigma-Aldrich	Cat# G2654; RRID: AB_259852
Rabbit anti-Insulin-647 (1:65)	Cell Signaling	Cat# 9008
Guinea pig anti-Insulin (1:1000)	Dako	Cat# A0564
Chicken anti-Insulin (1:10; flow cytometry)	Gallus Immunotech	Cat# ABI
Rabbit anti-MAFB (1:3000)	Gift from Roland Stein, Vanderbilt University	Cat# BL1228
Mouse anti-NKX2.2 (1:1000)	Developmental Studies Hybridoma Bank	Cat# 74-5A5; RRID: AB_531794
Rabbit anti-NKX6.1 (1:2000)	BCBC/Palle Serup	N/A
Rabbit anti-PDX1 (1:5000)	C. V. E. Wright	N/A
Goat anti-PDX1 (1:5000)	C. V. E. Wright	N/A
Goat anti-Somatostatin (1:500)	Santa Cruz	Cat# sc-7819; RRID: AB_2302603
Mouse anti-Somatostatin-AlexaFluor 488 (1:200; flow cytometry)	LS Bio	Cat# LS-C169129-100
Mouse anti-HIC3-2D12 (Hpa3; 1:200; flow cytometry)	Gift from Drs. Philip Streeter and Markus Grompe	N/A
Mouse anti-HIC0-4F9-Biotin (Hpi1; 1:100; flow cytometry)	Novus	Cat# NBP1-18872B RRID: AB_2126328
Donkey anti-chicken-APC (1:25; flow cytometry)	Jackson ImmunoResearch	Cat #703-136-155 RRID: AB_2340360
Donkey anti-goat-Alexa Flour 647 (1:200)	Jackson ImmunoResearch	Cat #705-605-003 RRID: AB_2340436
Donkey anti-Guinea pig-Cy2 (1:500)	Jackson ImmunoResearch	Cat #706-225-148 RRID: AB_2340467
Donkey anti-Guinea pig-Cy5 (1:200)	Jackson ImmunoResearch	Cat #706-175-148 RRID: AB_2340462
Donkey anti-mouse-Cy5 (1:200)	Jackson ImmunoResearch	Cat #715-175-151 RRID: AB_2340820
Donkey anti-rabbit-Cy3 (1:500)	Jackson ImmunoResearch	Cat #711-165-152 RRID: AB_2307443
Goat anti-mouse-PE (1:1000; flow cytometry)	BD Biosciences	Cat# 550589 RRID: AB_393768
Streptavidin BV421 (1:500; flow cytometry)	BD Biosciences	Cat# 563259
Biological Samples		
Human Pancreatic Islets (control and T1D)	Integrated Islet Distribution Program and Rita Bottino	
Human Pancreatic Tissue (control and T1D)	Rita Bottino	

Chemicals, Peptides, and Recombinant Proteins		
Propidium Iodide	BD Biosciences	Cat# 556463
Exenatide-4 (Ex-4)	California Peptide	Cat# 507-77
L-Arginine monohydrochloride	Sigma Life Science	Cat# A6969-25G; CAS: 001119-34-2
D-(+)-Glucose	Sigma Life Science	Cat# G7528-1KG; CAS: 50-99-7
3-Isobutyl-1-methylxanthine (IBMX)	Sigma Life Science	Cat# I5879-1G; CAS: 28822-58-4
(±)-Epinephrine-hydrochloride	Sigma-Aldrich	Cat# E4642-5G; CAS: 329-63-5
Potassium Chloride	Fisher Scientific	Cat# BP366-500; CAS: 7447-40-7
Collagenase NB1 Premium Grade	Crescent Chemical	Cat# 17455.03
Neutral Protease NB1 Premium Grade	Crescent Chemical	Cat# 30301.02
DNase I	Worthington Biochemical Corporation	Cat# LS006333
RPMI Medium	Mediatech	99-595-CM
Biocoll-Separating Solution, Density 1.10 g/mL	Cedarlane	Cat# L6155
Biocoll-Separating Solution, Density 1.077 g/mL	Cedarlane	Cat# L6113
Fetal Calf Serum	Life Technologies	Cat# 16-140-071
Dithizone	Sigma	Cat# D5130
CMRL 1066 Medium	Mediatech	Cat# 99-663-CV
Penicillin/Streptomycin mix	Life Technologies	Cat# 15140163
L-glutamine	Life Technologies	Cat# 2030-081
16% paraformaldehyde	Electron Microscopy Sciences	Cat# 15710
O.C.T. compound	Fisher Scientific	Cat# 4585
Critical Commercial Assays		
Insulin Radioimmunoassay	Millipore	RI-13K
Glucagon Radioimmunoassay	Millipore	GL-32K
RNAqueous-Microkit	Invitrogen by Thermo Fisher Scientific	AM1931
EIA ELISA	Phoenix Pharmaceuticals	EK-070-94
Human-specific insulin radioimmunoassay	Millipore	HI-14K
Deposited Data		
RNA-seq data for FACS purified human control and T1D alpha cells	NCBI Gene Expression Omnibus	GEO: GSE106148
Experimental Models: Organisms/Strains		
Mouse: NOD-*scid-IL2rγ*^{null} (NSG)	Jackson Laboratory	https://www.jax.org/strain/005557
Oligonucleotides		
18S	Applied Biosystems	Hs99999901_s1
ACTB	Applied Biosystems	Hs99999903_m1
ARX	Applied Biosystems	Hs00292465_m1
GCG	Applied Biosystems	Hs00174967_m1
INS	Applied Biosystems	Hs02741908_m1
MAFA	Applied Biosystems	Hs01651425_s1
MAFB	Applied Biosystems	Hs00534343_s1
NKX2.2	Applied Biosystems	Hs00159616_m1

NKX6.1	Applied Biosystems	Hs00232355_m1
PDX1	Applied Biosystems	Hs00236830_m1
Software and Algorithms		
TopHat (v2.1)	Trapnell, 2009	http://tophat.cbcb.umd.edu/ RRID: SCR_013035
Avadis NGS analysis Platform	Strand life Sciences, Bengaluru	http://www.avadis-ngs.com RRID: SCR_000644
Trimmed Mean of M-values (TMM) algorithm	Dillies, 2012 Robinson, 2010	
DAVID (v6.8)	Huang, 2009	http://david.abcc.ncifcrf.gov/ RRID: SCR_001881
Ingenuity Pathway Analysis (IPA)	Qiagen	RRID: SCR_008653
Prism v.7.0	Graphpad Software	https://www.graphpad.com; RRID: SCR_002798
MetaMorph 7.1	Molecular Devices	https://www.moleculardevices.com; RRID: SCR_002368
Zeiss LSM Imaging Software (confocal)	Carl Zeiss	https://www.zeiss.com; RRID: SCR_014344
Genome Analysis Toolkit (GATK) HaploTypeCaller v3.3	Broad Institute	https://software.broadinstitute.org/gatk/; RRID: SCR_001876
Other		
Zenon Kit Alexa Fluor 488	Invitrogen	Cat# Z25002
Zenon Kit Pacific Blue	Invitrogen	Cat# Z25041
Tyramide Signal Amplification	Perkin Elmer	Cat# NEL744001KT

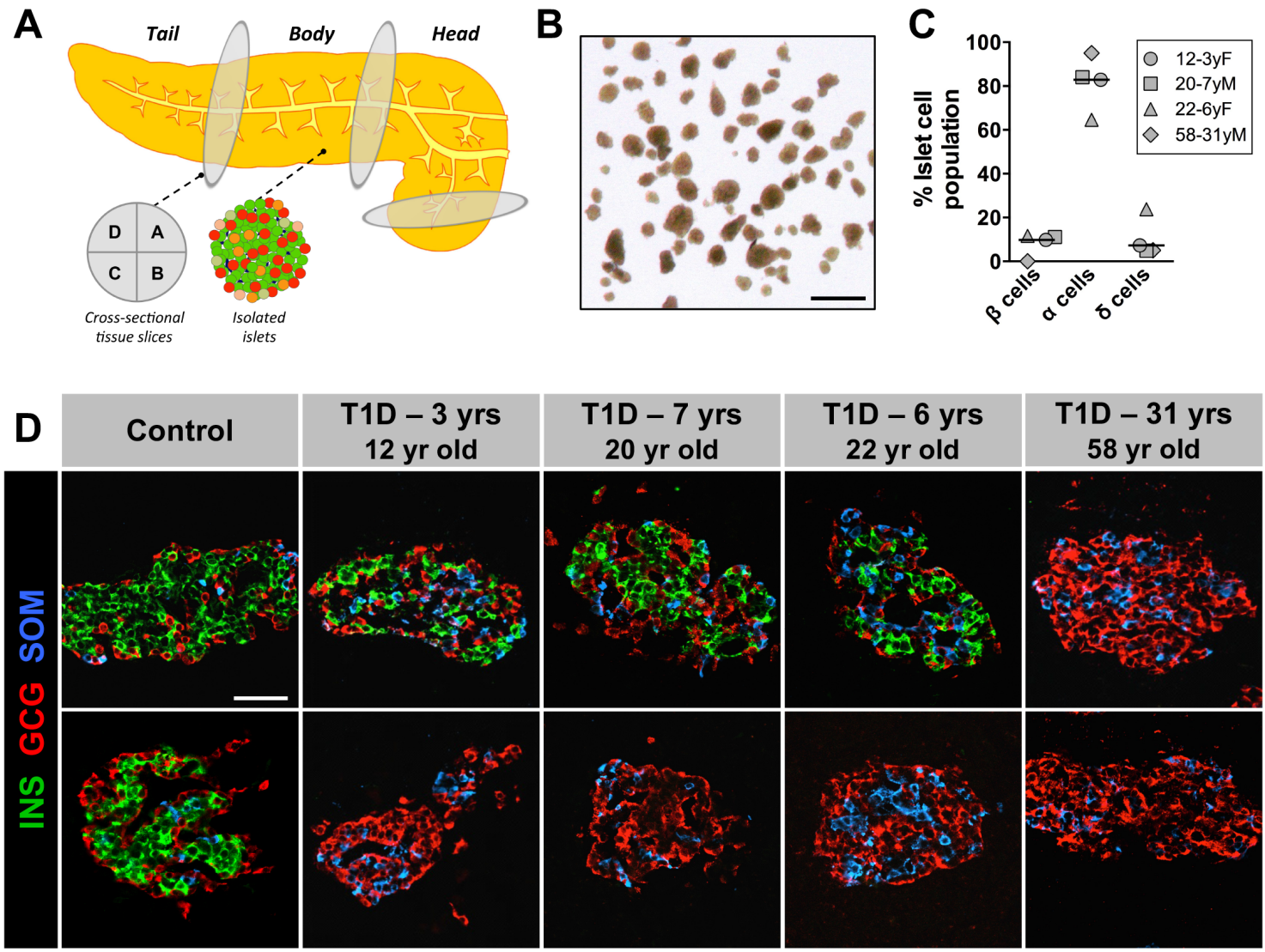

Figure S1. Related to Figures 1 and 2. Composition and morphology in T1D islets. (**A**) Schematic of islet isolation and tissue procurement from the same pancreas. Prior to islet isolation, multiple cross-sectional slices of pancreas with 2-3 mm thickness were obtained from the head, body and tail. Pancreatic slices were further divided into four quadrants (*A, B, C, D*) and processed for histology. (**B**) Pancreatic islets procured from a 12-year-old individual with 3-year T1D duration (donor #1). (**C**) Endocrine cell populations in dispersed isolated islets from 3 donors (#1,4,5) with recent-onset T1D contained 10.8±0.5% β cells, 77.1±6.3% α cells, and 12.0±5.9% δ cells. The donor with longstanding T1D (donor #8) had 0% β cells, 95% α cells, and 5% δ cells. For comparison, islets from normal individuals (n=28) with average age of 36±2 years (range 16 – 63 years) assessed by this approach had 53.4±2.6% β cells, 38.5±2.7% α cells, and 7.5±0.9% δ cells (Blodgett et al., 2015). (**D**) Morphology of T1D islets in the native pancreas. On average 250 islets from pancreatic head, body and tail of each T1D donor were analyzed for the presence of β cells. An islet was categorized as insulin+ even if it had only one insulin-positive cell. The number of insulin+ islets varied in 4 donors (#1,3,4,5) with recent-onset T1D (17.8±15.5%), but no insulin+ islets were found in the pancreatic sections of our longstanding cases (donors #6,7,8). If donors had insulin+ islets, representative islets are displayed in row 1. INS–insulin, GCG–glucagon, SOM–somatostatin. Scale bar is 50 μm.

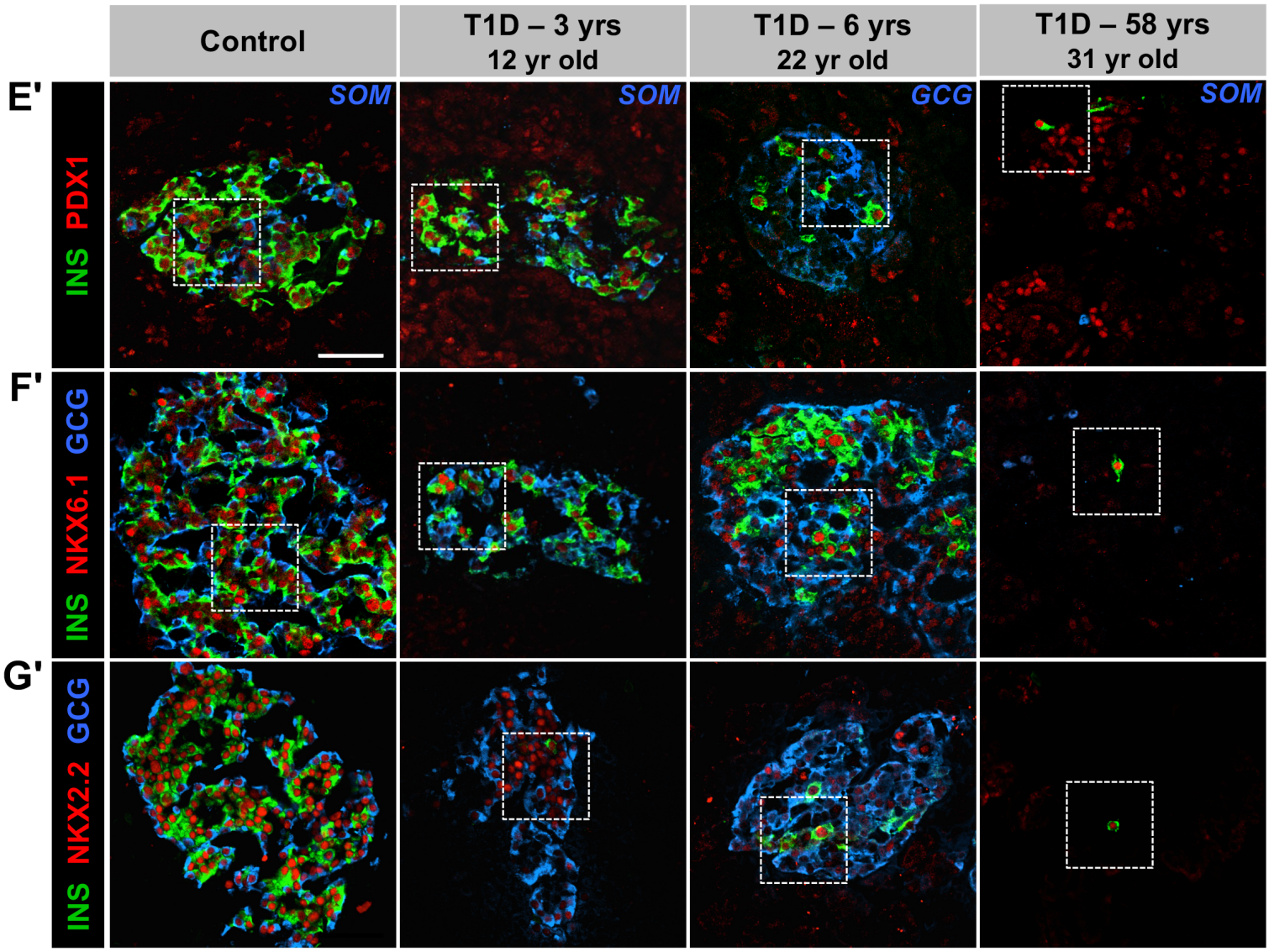

Figure S2. Related to Figure 1. Expression pattern of PDX1, NKX6.1, and NKX2.2 in T1D β cells. Expression of β cell-enriched transcription factors in the native pancreatic tissue from donors with recent-onset T1D (donors #1,5) was compared to 58-year-old donor with 31 years of T1D duration (donor #8) and controls. INS–insulin, GCG–glucagon, SOM–somatostatin. Regions denoted by the dashed line in panels **E'**– **G'** are displayed in panels **E** – **G** in **Figure 1**, respectively. Scale bar in **E'** is 50 μm and also corresponds to panels **F'** and **G'**.

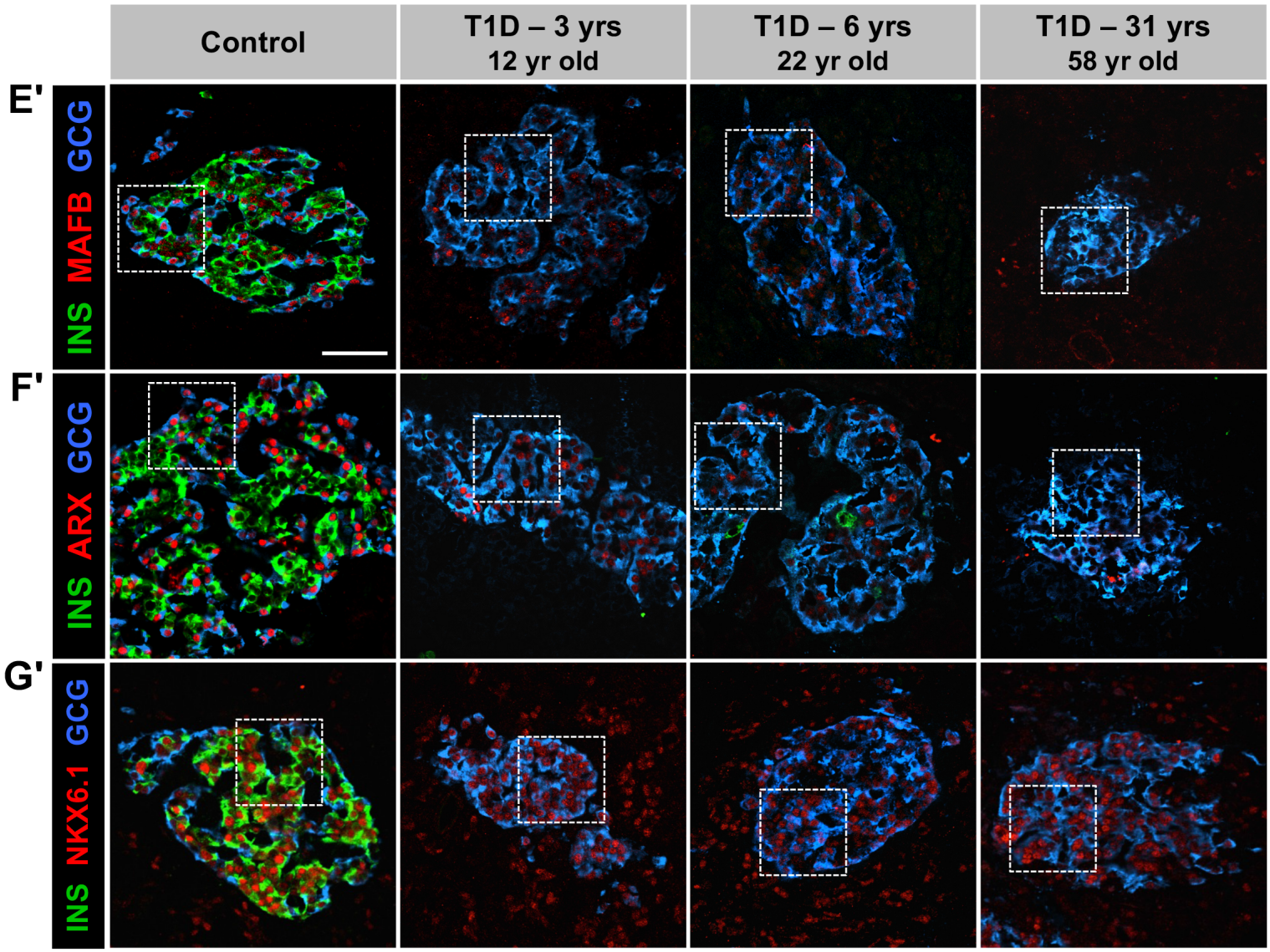

Figure S3. Related to Figure 2. Expression pattern of MAFB, ARX, and NKX6.1 in T1D α cells. Expression of α cell-enriched transcription factors in the native pancreatic tissue from donors with recent-onset T1D (donors #1,2,5) was compared to 58-year-old donor with 31 years of T1D duration and controls (donor #8). GCG–glucagon, SOM–somatostatin. Regions denoted by the dashed line in panels **E'**–**G'** are displayed in panels **E**–**G** in **Figure 2**, respectively. Scale bar in **E'** is 50 μm and also corresponds to panels **F'** and **G'**.

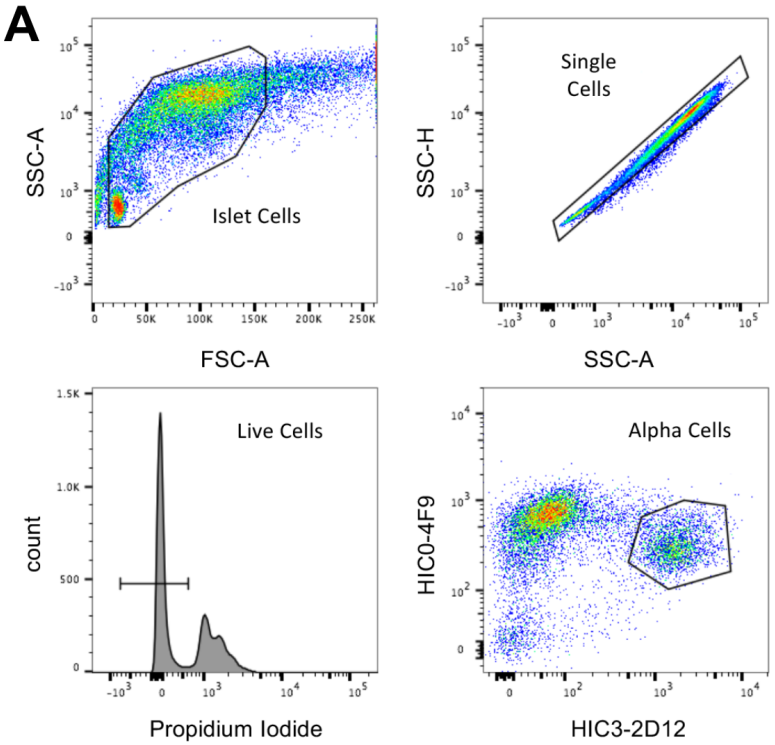
A
SSC-A
FSC-A
Islet Cells
SSC-H
SSC-A
Single Cells
count
Propidium Iodide
Live Cells
HIC0-4F9
HIC3-2D12
Alpha Cells

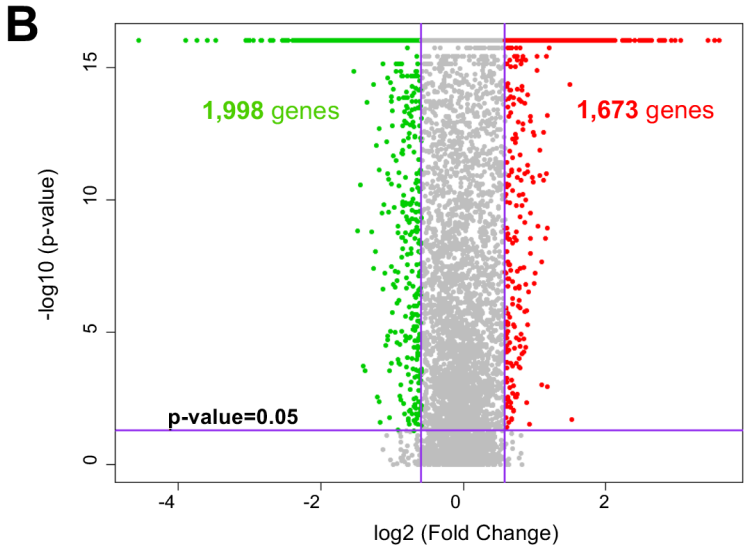
B
-log10 (p-value)
log2 (Fold Change)
1,998 genes
1,673 genes
p-value=0.05

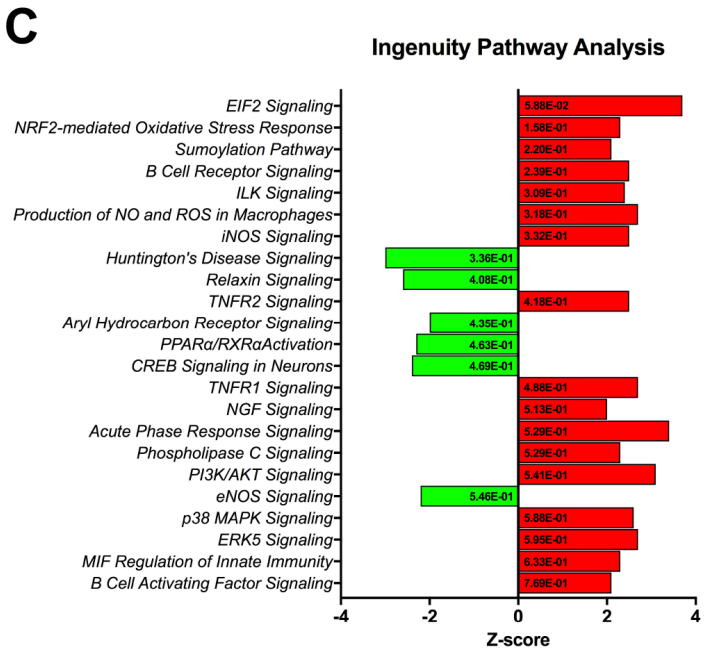
C
Ingenuity Pathway Analysis
EIF2 Signaling
NRF2-mediated Oxidative Stress Response
Sumoylation Pathway
B Cell Receptor Signaling
ILK Signaling
Production of NO and ROS in Macrophages
iNOS Signaling
Huntington's Disease Signaling
Relaxin Signaling
TNFR2 Signaling
Aryl Hydrocarbon Receptor Signaling
PPARα/RXRαActivation
CREB Signaling in Neurons
TNFR1 Signaling
NGF Signaling
Acute Phase Response Signaling
Phospholipase C Signaling
PI3K/AKT Signaling
eNOS Signaling
p38 MAPK Signaling
ERK5 Signaling
MIF Regulation of Innate Immunity
B Cell Activating Factor Signaling
5.88E-02
1.58E-01
2.20E-01
2.39E-01
3.09E-01
3.18E-01
3.32E-01
3.36E-01
4.08E-01
4.18E-01
4.35E-01
4.63E-01
4.69E-01
4.88E-01
5.13E-01
5.29E-01
5.29E-01
5.41E-01
5.46E-01
5.88E-01
5.95E-01
6.33E-01
7.69E-01
Z-score

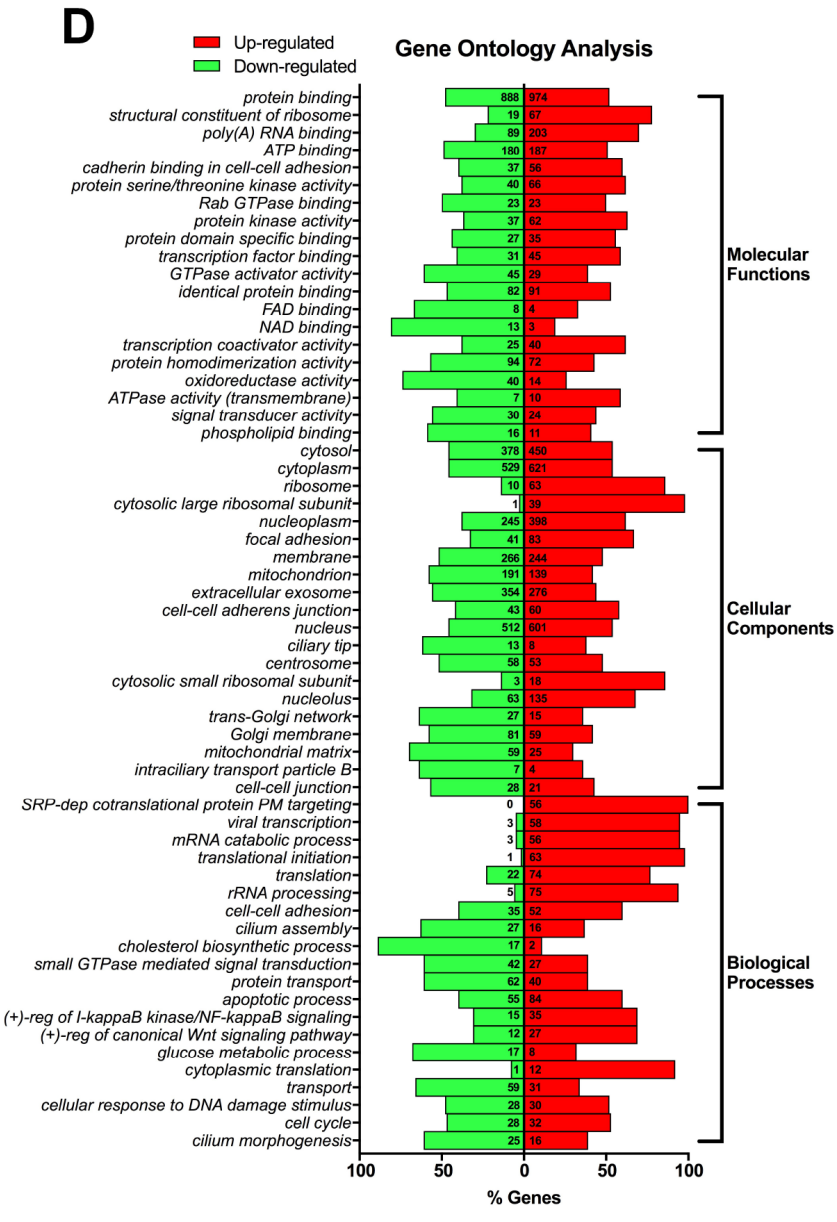
D
Up-regulated
Down-regulated
Gene Ontology Analysis
protein binding
structural constituent of ribosome
poly(A) RNA binding
ATP binding
cadherin binding in cell-cell adhesion
protein serine/threonine kinase activity
Rab GTPase binding
protein kinase activity
protein domain specific binding
transcription factor binding
GTPase activator activity
identical protein binding
FAD binding
NAD binding
transcription coactivator activity
protein homodimerization activity
oxidoreductase activity
ATPase activity (transmembrane)
signal transducer activity
phospholipid binding
cytosol
cytoplasm
ribosome
cytosolic large ribosomal subunit
nucleoplasm
focal adhesion
membrane
mitochondrion
extracellular exosome
cell-cell adherens junction
nucleus
ciliary tip
centrosome
cytosolic small ribosomal subunit
nucleolus
trans-Golgi network
Golgi membrane
mitochondrial matrix
intraciliary transport particle B
cell-cell junction
SRP-dep cotranslational protein PM targeting
viral transcription
mRNA catabolic process
translational initiation
translation
rRNA processing
cell-cell adhesion
cilium assembly
cholesterol biosynthetic process
small GTPase mediated signal transduction
protein transport
apoptotic process
(+)-reg of I-kappaB kinase/NF-kappaB signaling
(+)-reg of canonical Wnt signaling pathway
glucose metabolic process
cytoplasmic translation
transport
cellular response to DNA damage stimulus
cell cycle
cilium morphogenesis
Molecular Functions
Cellular Components
Biological Processes
% Genes

Figure S4. Related to Figure 4. Transcriptome analysis of purified human α cells by RNA-sequencing. (**A**) Gating strategy for sorting of dispersed human islet cells by Fluorescence Activated Cell Sorting (FACS). Cell debris was excluded by forward scatter (FSC) and side scatter (SSC), single cells were identified by SSC-H v. SSC-A plot, and non-viable cells were excluded using Propidium Iodide (PI). The α cell population was isolated based on double positivity for HIC3-2D12 (Hpa3) and HIC0-4F9 (Hpi1) antibodies. (**B**) Volcano plot displays transcripts differentially expressed between control and T1D samples (donors #3,6,7) that reached statistical significance (upregulation: red; downregulation: green). Differential expression between the two sample sets was calculated on the basis of FC (≥1.5) with a <0.05 p-value cut-off for calculated z-score. (**C**) Graph represents the top 20 most significantly (z-score >2 or <-2) altered canonical pathways identified by Ingenuity Pathway Analysis (IPA) with corresponding p-value depicted on graph bar. Pathways with affiliated Ensembl Gene Stable IDs are listed in **Table S3**. (**D**) Bar graph highlights the percentage of up- and down-regulated genes (with corresponding gene number displayed within bar) in the top 20 significant biological processes, cellular components, and molecular functions identified by Gene Ontology (GO) term analysis. Corresponding p-values, Ensembl Gene Stable IDs and process GO accession numbers are listed in **Table S4.**

Table S1. Related to Figures 1-4. Demographic information of normal donors

Donors	Age (years)	Ethnicity/ Race	Gender	BMI	Cause of Death	Tissue/Islet Source
Normal Controls for Islet Perifusion	7	Caucasian	M	26.8	Respiratory arrest	Rita Bottino
	8	Caucasian	F	16.1	Intracerebral hemorrhage	Rita Bottino
	8	African American	M	17.2	Anoxia	Rita Bottino
	9	Caucasian	M	15.5	Head Trauma	Rita Bottino
	11	African American	M	18.3	Anoxia	Rita Bottino
	19	Caucasian	M	20.1	Head Trauma	Rita Bottino
	19	Caucasian	M	34.1	Head Trauma	IIDP
Normal Controls for Islet Transplants	20	African American	M	21.7	Head Trauma	IIDP
	39	N/A	F	28.2	N/A	IIDP
	53	Native Hawaiian or Other Pacific Islander	F	25.4	N/A	IIDP
Normal Control for qRT-PCR	11	Caucasian	M	22.7	Anoxia	Rita Bottino
	20	Hispanic/ Latino	F	24.6	Anoxia	IIDP
	29	Hispanic/ Latino	M	27.5	Head Trauma	IIDP
Normal Controls for Histology	8	African American	M	17.2	Anoxia	Rita Bottino
	10	Caucasian	M	19.3	Head Trauma	Rita Bottino
	19	Caucasian	M	20.1	Head Trauma	Rita Bottino
	19	Caucasian	M	21.2	Anoxia	Rita Bottino
	20	Hispanic/ Latino	M	19.4	Head Trauma	Rita Bottino
	24	Caucasian	M	35.5	Head Trauma	Rita Bottino
	55	African American	M	35.6	Stroke	Rita Bottino
Normal Controls for RNA-seq	26	Hispanic/Latino	F	35.9	Anoxia	IIDP
	35	Caucasian	F	23.6	Anoxia	IIDP
	49	Caucasian	F	31.6	Stroke	IIDP
	50	African American	M	30.2	Stroke	IIDP
	55	Caucasian	M	27.8	Stroke	IIDP

N/A – not available; IIDP – Integrated Islet Distribution Program

Table S2. Related to Figures 1- 4 and Table 1. DNA sequencing of T1D donors for variants associated with monogenic diabetes

Donor	Gene	Chr	Transcript	Nucleotide	Amino Acid Change	dbSNP ID	MAF	POLY Score
1	*AKT2*	19	NM_001626.5	c.*9C>T	-	rs79275829	0.004	0
	CYP27B1	12	NM_000785.3	c.963+2T>G	-	-	0	0
	CYP27B1	12	NM_000785.3	c.963+7T>G	-	-	0	0
	FOXP3	X	NM_014009.3	c.403A>C	p.Thr135Pro	-	0	0
	IFIH1	2	NM_022168.3	c.1641+1G>C	-	rs35337543	0.007	0
	SIRT1	10	NM_012238.4	c.110C>T	p.Pro37Leu	-	0	0.013
	GLP1R	6	NM_002062.3	c.1347G>A	p.Ala449Ala	rs201020486	0	0
2	*AIRE*	21	NM_000383.3	c.1411C>T	p.Arg471Cys	rs74203920	0.006	0.997
	ALMS1	2	NM_015120.4	c.69_77del	p.Glu27_Glu29del	-	0	0
	HSD11B1	1	NM_005525.3	c.219+6G>A	-	rs202219444	0	0
	LRBA	4	NM_006726.4	c.1536A>G	p.Ser512Ser	-	0	0
	POMC	2	NM_001035256.1	c.706C>G	p.Arg236Gly	rs28932472	0.004	1
	PTPN22	1	NM_015967.5	c.1508A>G	p.Tyr503Cys	rs371916399	0	0.004
	TBC1D4	13	NM_014832.3	c.2913A>T	p.Gly971Gly	rs184774790	0	0
3	*BBS5*	2	NM_152384.2	c.620G>A	p.Arg207His	rs35487251	0.006	0.833
	BLM	15	NM_000057.3	c.2119C>T	p.Pro707Ser	rs146077918	0.001	0.018
	EIF2AK3	2	NM_004836.5	c.-201A>G	-	rs144057685	0.005	0
	HFE	6	NM_000410.3	c.845G>A	p.Cys282Tyr	rs1800562	0.02	0
	HNF4A	20	NM_175914.4	c.1314C>G	p.Leu438Leu	-	0	0
	PIK3R1	5	NM_181523.2	c.1176C>T	p.Phe392Phe	rs3730090	0.308	0
4	*ALMS1*	2	NM_015120.4	c.12278G>A	p.Arg4093His	-	0	0
	FBN1	15	NM_000138.4	c.3294C>T	p.Asp1098Asp	rs140587	0.008	0
	GLP1R	6	NM_002062.3	c.59G>A	p.Arg20Lys	rs10305421	0.007	0.643
	IFIH1	2	NM_022168.3	c.1075G>C	p.Val359Leu	-	0	0.996
	MKS1	17	NM_017777.3	c.1528C>T	p.Arg510Trp	-	0	0.976

5	*BLM*	15	NM_000057.3	c.2268A>G	p.Lys756Lys	rs146013879	0.001	0
	CLEC16A	16	NM_015226.2	c.2945G>A	p.Ser982Asn	rs72650689	0.004	0.967
	HFE	6	NM_000410.3	c.187C>G	p.His63Asp	rs1799945	0.084	0
	LRBA	4	NM_006726.4	c.7597A>C	p.Thr2533Pro	rs62346982	0.003	0.167
	KCNK16	6	NM_032115.3	c.165G>A	p.Leu55Leu	rs138076469	0.002	0
	LMNA	1	NM_005572.3	c.612G>A	p.Leu204Leu	rs12117552	0.004	0
6	*ABCC8*	11	NM_000352.4	c.-430C>T	-	-	0	0
	BBS2	16	NM_031885.3	c.155T>A	p.Val52Asp	-	0	0.016
	EIF2AK3	2	NM_004836.5	c.-201A>G	-	rs144057685	0.005	0
	MKKS	20	NM_018848.3	c.1015A>G	p.Ile339Val	rs137853909	0.001	0.008
	NTRK2	9	NM_006180.4	c.483T>G	p.Thr161Thr	rs199849633	0	0
	VPS13B	8	NM_017890.4	c.8978A>G	p.Asn2993Ser	rs28940272	0.002	0.997
7	*ABCC8*	11	NM_000352.4	c.2176G>A	p.Ala726Thr	rs138687850	0.001	0.02634
	AKT2	19	NM_001626.5	c.1110G>T	p.Pro370Pro	rs41309435	0.001	0
	CFTR	7	NM_000492.3	c.1521_1523del	p.Phe508del	rs199826652	0.006	0
	LRBA	4	NM_006726.4	c.217-10del	-	-	0	0
	VPS13B	8	NM_017890.4	c.1832G>A	p.Arg611Lys	rs61754109	0	0.02634
8	*AKT2*	19	NM_001626.5	c.945G>A	p.Glu315Glu	rs150000674	0.002	0
	CYP27B1	12	NM_000785.3	c.963+2T>G	-	-	0	0
	CYP27B1	12	NM_000785.3	c.963+7T>G	-	-	0	0
	FXN	9	NM_000144.4	c.-7G>A	-	rs145006100	0.011	0
	IFIH1	2	NM_022168.3	c.1641+1G>C	-	rs35337543	0.007	0

Chr – Chromosome, MAF – Minor allele frequency; DNA isolated from pancreatic samples of T1D donors was subjected to DNA sequencing covering coding regions and splice junctions of 148 genes associated with monogenic diabetes.

SUPPLEMENTAL REFERENCES

Aamodt, K.I. et al., 2016. Development of a reliable automated screening system to identify small molecules and biologics that promote human β-cell regeneration. *American journal of physiology Endocrinology and metabolism*, 311(5), pp.E859–E868.

Alkorta-Aranburu, G. et al., 2016. Improved molecular diagnosis of patients with neonatal diabetes using a combined next-generation sequencing and MS-MLPA approach. *Journal of pediatric endocrinology & metabolism : JPEM*, 29(5), pp.523–531.

Benjamini, Y. & Hochberg, Y., 1995. A direct approach to false discovery rates. *J. Royal Stat. Soc., Ser. B*, 57(1), pp.289–300.

Blodgett, D.M. et al., 2015. Novel Observations From Next-Generation RNA Sequencing of Highly Purified Human Adult and Fetal Islet Cell Subsets. *Diabetes*, 64(9), pp.3172–3181.

Brissova, M. et al., 2014. Islet microenvironment, modulated by vascular endothelial growth factor-A signaling, promotes β cell regeneration. *Cell metabolism*, 19(3), pp.498–511.

Dillies, M.-A. et al., 2012. A comprehensive evaluation of normalization methods for Illumina high-throughput RNA sequencing data analysis. *Briefings in bioinformatics*.

Dorrell, C. et al., 2016. Human islets contain four distinct subtypes of β cells. *Nature communications*, 7, p.11756.

Huang, D.W. et al., 2009. Extracting biological meaning from large gene lists with DAVID. *Current protocols in bioinformatics*, Chapter 13, p.Unit 13.11.

Kayton, N.S. et al., 2015. Human islet preparations distributed for research exhibit a variety of insulin-secretory profiles. *American journal of physiology Endocrinology and metabolism*, 308(7), pp.E592–602.

Malone, J.H. & Oliver, B., 2011. Microarrays, deep sequencing and the true measure of the transcriptome. *BMC biology*, 9, p.34.

Robinson, M.D. & Oshlack, A., 2010. A scaling normalization method for differential expression analysis of RNA-seq data. *Genome biology*, 11(3), p.R25.

Trapnell, C., Pachter, L. & Salzberg, S.L., 2009. TopHat: discovering splice junctions with RNA-Seq. *Bioinformatics (Oxford, England)*, 25(9), pp.1105–1111.